Journal of Inclusion Phenomena and Molecular Recognition in Chemistry **21**: 159–184, 1995.

Zeolite Encapsulated Metal Complexes

KENNETH J. BALKUS, Jr. and ALEXEI G. GABRIELOV

1. Introduction

The potential for coupling the shape selectivity associated with the well-defined channels and cages of zeolites with the reactivity of metal complexes makes these molecular sieves particularly attractive as solid supports. Zeolites have a distinct advantage over conventional support materials in that a metal complex can be physically trapped in the pores and not necessarily bound to the oxide surface. A metal complex of the appropriate dimensions might be encapsulated in a zeolite yet be free to move within the confines of a cage or channel. This could be viewed as a bridge between a homogeneous and heterogeneous system. Herron et al. [1] first referred to such zeolite guest molecules as ship-in-a-bottle complexes. This term has become quite popular in describing zeolite-encapsulated metal chelates and cluster complexes. The novel reactivity that was anticipated for zeolite ship-in-a-bottle complexes is gradually being realized as efforts in this area grow. In particular, progress in the area of biomimetic chemistry such as dioxygen binding and oxidation catalysis has elicited the terms inorganic protein [2,3] and zeozyme [4] to describe certain zeolite encapsulated metal complexes. In this context, even silicon-based life has been contemplated [5].

Romanovsky et al. first reported the synthesis of a metal phthalocyanine (MPc) inside zeolite Na-Y in 1977 [6-9]. Since then several groups have studied the encapsulation and reactivity of MPc complexes [3,4,6-52] as well as related porphyrins [23,51,53,54] in zeolite molecular sieves. The MPc complex is trapped in a zeolite cavity that has restricted apertures and provides a good example of a ship-in-a-bottle complex. The tetradentate Schiff base ligand N,N'-bis(salicylidene)ethylenediimine or SALEN has also been complexed in synthetic faujasite type zeolites [2,55-62]. Ship-in-a-bottle complexes are not limited to large chelates. For example, bis(cyclopentadienyl)cobalt(III) ion can be encapsulated in Nonasil, a clathrasil type molecular sieve, during synthesis [63,64]. Therefore, the only limitation as to the nature of the zeolite and metal complex is the method of encapsulation. In this chapter, we hope to review the synthetic strategies and characterization techniques for zeolite encapsulated metal complexes as well as give a brief summary of emerging applications. In many cases, parallel studies of simple intrazeolite coordination complexes have also been shown to be quite promising but this area has been more frequently reviewed [65,66] and will not be addressed here. Likewise, zeolite supported bulk metal particles [67,68] as well as metal oxides [69] have

been omitted from this review.

2. Synthesis of Zeolite Encapsulated Complexes

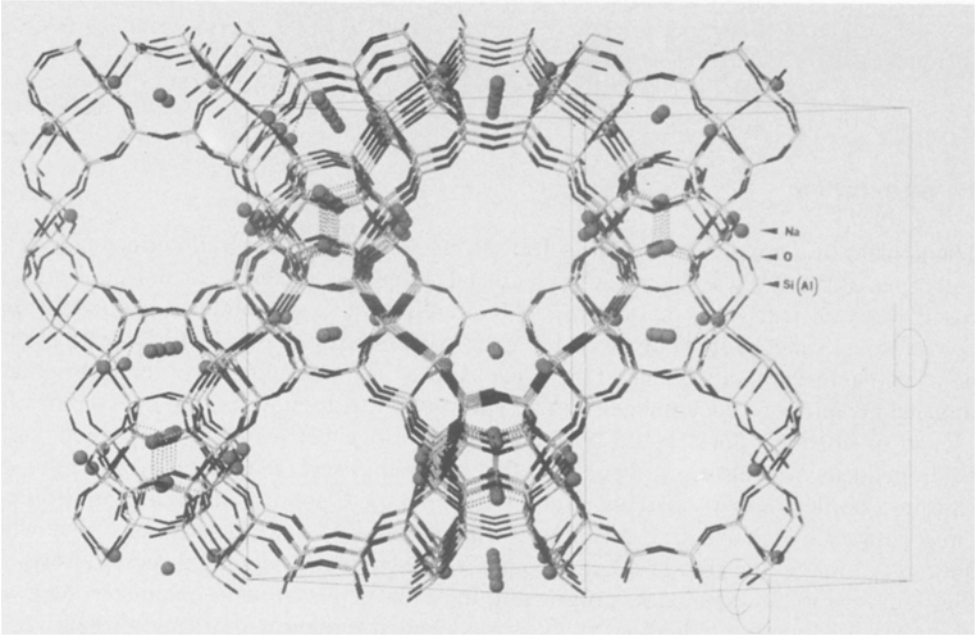

Figure 1. A [110] view of zeolite Na-Y.

There are four general strategies for the encapsulation of metal complexes in molecular sieves that include,

(i) the in situ preparation of intrazeolite metal carbonyl clusters;
(ii) the flexible ligand method;
(iii) the template synthesis method;
(iv) the zeolite synthesis method.

The first three methods generally involve large pore zeolites and molecular sieves. The synthetic faujasite type (FAU) zeolites X and Y have a three-dimensional pore system with ~7.4 Å channels that open up to supercages 12 Å in diameter [70] as shown in Figure 1. From this structure one can envision an intrazeolite metal complex that is small enough to fit inside the supercage but is effectively larger than the cavity openings. Metal complexes have also been encapsulated in VPI-5 (VFI) type molecular sieves shown in Figure 2 which have a one-dimensional channel system with a fixed diameter of 12.1 Å. In the case of metal phthalocyanines, these large complexes are probably wedged in the slightly smaller channels.

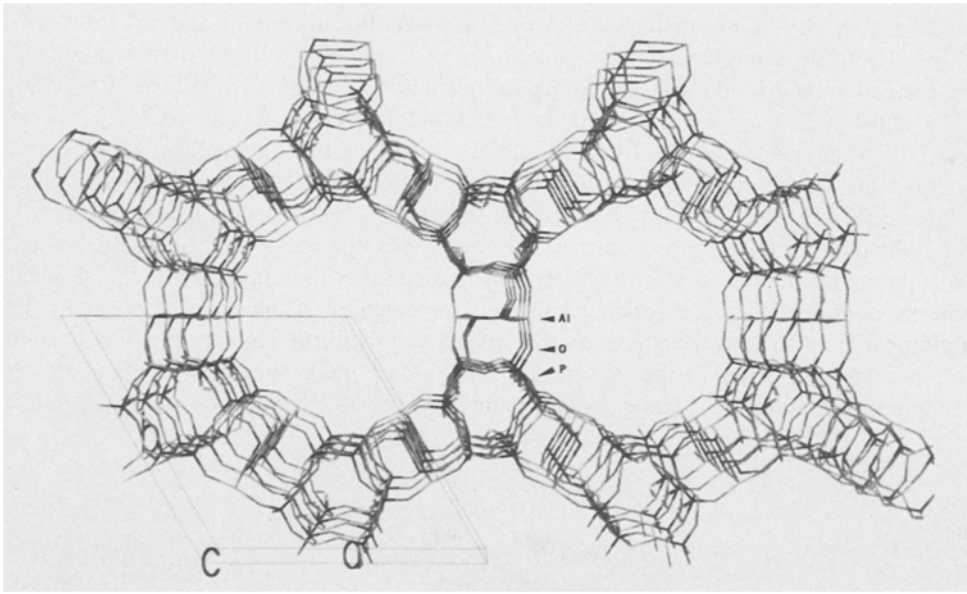

Figure 2. A [001] view of the aluminum phosphate molecular sieve VPI-5.

The encapsulation methods that involve preparing a complex inside a zeolite are limited by the ability to diffuse reagents into the crystalline molecular sieve. Zeolites such as Na-A, which has a large cavity 11.9 Å in diameter but openings that are only 4.1 Å, can not be modified with most ligands or ligand precursors because of the size restrictions of the cage windows. However, if the zeolite is synthesized around the metal complex, then only the cage dimensions are important as far as ligand size is concerned. In this case, the metal complex must meet the requirement of stability during crystallization but this is not a major restriction since zeolites/molecular sieves can be synthesized under many conditions that include low pH fluoride syntheses, high pH hydroxide mediated synthesis, and crystallizations from non-aqueous solvents. The zeolite synthesis approach has been employed to encapsulate metal complexes in a variety of molecular sieves ranging from the small pore clathrasils to the large pore FAU type zeolites. We next briefly review key examples of encapsulated metal complex syntheses before discussing their characterization and reactivity. For a more detailed discussion of synthesis techniques see Chapter 7 by Schoonheydt et al. in this volume.

2.1 METAL CLUSTER SYNTHESIS

Metal carbonyl adducts probably constitute the most widely studied group of intrazeolite

coordination complexes [71]. Metal carbonyl clusters with a nuclearity greater than three could potentially be encapsulated in a FAU type zeolite, forming a special subclass of ship-in-a-bottle complexes. The reaction of CO/H_2 or CO/H_2O with a metal ion-exchanged Y type zeolite has lead to the encapsulation of $Rh_6(CO)_{16}$ [72-76], $Rh_4(CO)_{12}$ [76], and $Ir_4(CO)_{12}$ [76], as well as the bimetallic derivatives $Rh_{6-x}Ir_x(CO)_{16}$ (x= 0-6) [77,78]. Figure 3 shows the $Rh_6(CO)_{16}$ entrapped in a FAU supercage which clearly leaves considerable room in the cavity. In fact, clusters as large as $Pd_{13}(CO)_X$ have been characterized in Na-Y zeolites [79,80]. The presence of H_2 or H_2O appears necessary for the reductive carbonylation of intrazeolite metal ions and the formation of the clusters. An interesting feature of the cluster synthesis method is the apparent ease with which anionic complexes can be generated in the supercages of X and Y type zeolites. The aluminosilicate framework is negatively charged and therefore anions should be unstable in the channels. Some of the first intrazeolite anionic metal species were generated by complexation with the strong field ligand cyanide to produce complexes such as

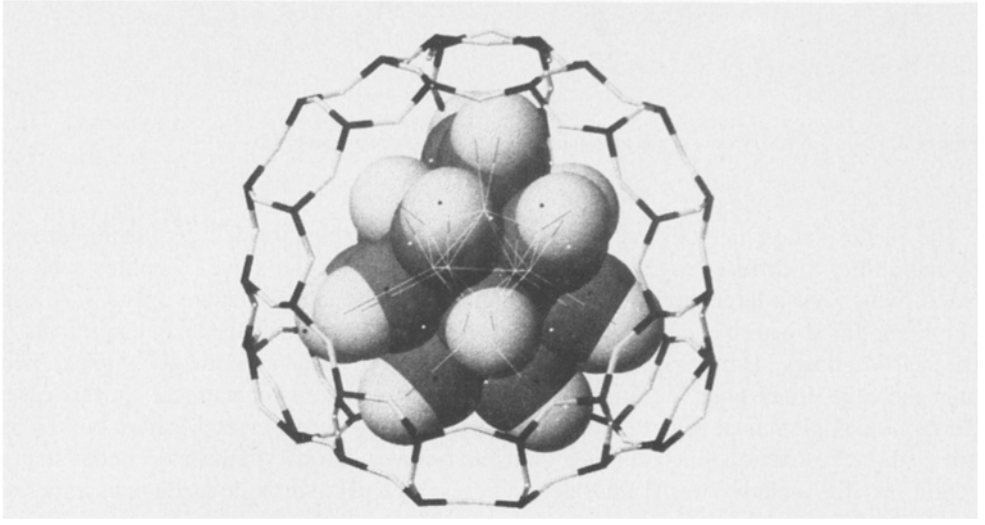

Figure 3. A space filling model of $Rh_6(CO)_{16}$ in a Na-Y supercage.

$Co(CN)_4^{2-}$ [81-83] and $Fe(CN)_4^{2-}$ [84]. Although, charge formalism is not as straightforward, anionic clusters of the type $[HFe_3(CO)_{11}]^-$ [77,78,85], $[HOs_3(CO)_{11}]^-$ [86,87], $[Ir_6(CO)_{15}]^{2-}$ [88,89], $[Co_6(CO)_{15}]^{2-}$ [90], and the Chini-type complexes $[Pt_3(CO)_3(\mu_2\text{-}CO)_3]_n^{2-}$ (n =3,4,5) [91-94] have been characterized in Na-Y zeolites. A bimetallic cluster, $[Rh_4Fe_2(CO)_{16}]^{2-}$, has been prepared in Na-Y by the reaction of

CO/H_2 with Rh(III)/Fe(II) exchanged zeolite or by the reaction of $Rh_4(CO)_{12}$ with encapsulated $[HFe_3(CO)_{11}]^-$ [77,78]. The question becomes why are these anionic clusters stable within the anionic zeolite lattice? In fact, the trinuclear species are not physically precluded from exiting the supercage. Also, the migration and aggregation of "$Pt_3(CO)_6$" species have been mechanistically implicated in the formation of encapsulated Chini complexes [94]. Therefore, certain trinuclear clusters may not be entrapped. However, the 12-ring windows to the supercage are defined by oxygens that bear partial negative charge. Passage of anions through this aperture is unfavorable so that the smaller anionic clusters may be electrostatically trapped. Additionally, the bifunctional activation of carbon monoxide, which arises from the interaction of a metal bound carbonyl with a charge balancing cation, may stabilize the intrazeolite cluster.

Molecular precursors such as $Ir(CO)_2(acac)$ may be absorbed into the zeolite and then reacted with CO to form encapsulated $Ir_4(CO)_{12}$ [95,96] or with CO/H_2 to give $Ir_6(CO)_{16}$ [97]. $Co_2(CO)_8$ absorbed in Na-Y leads to encapsulated $Co_4(CO)_{12}$ [98]. The numerous possibilities for molecular precursors to carbonyl clusters dramatically expands the potential for new and interesting intrazeolite species.

2.2 FLEXIBLE LIGAND METHOD

The flexible ligand method involves the diffusion of a multidentate ligand into the zeolite pores where, upon complexation with a metal ion, it becomes too large to exit. This approach is typified by the encapsulation of metal-SALEN complexes in synthetic faujasite type zeolites. Figure 4 illustrates how the free SALEN ligand might diffuse through the 12-ring windows and complex a supercage metal ion. The encapsulated MSALEN complex is sterically constrained to the supercage. However, computer modeling suggests that a MSALEN species might be able to squeeze itself back out [58]. Nevertheless, encapsulated SALEN complexes of Co [2,59,60], Fe [61], Mn [55,61], Rh [56], Ru [62], and Pd [57,58] have been reported. Typically, a dehydrated or partially dehydrated metal ion exchanged X or Y type zeolite is slurried with the melted SALEN free base ligand. Subsequently, the SALEN modified zeolite is solvent extracted to remove surface species.

The SALEN ligand generally binds in a tetradentate fashion. However, SALEN may also bind one or more metals in a bidentate fashion. Additionally, the ligand may bind in other than a square planar geometry depending upon what else is bound to the metal ion. The nature of the encapsulated SALEN complexes is not clear from spectroscopic data. This is further complicated by the presence of free base ligand as well as uncomplexed metal ions. In the case of Co(II)SALEN encapsulated in Na-Y, cyclic voltammetry has revealed the presence of two intrazeolite complexes [60]. One complex binds added base, such as pyridine, while the other is unreactive. This may be a consequence of different structural isomers or more likely different modes of coordination. Not all the MSALEN complexes behave in this fashion. For example, the higher oxidation state Mn(III)SALEN exhibits only one form inside Na-Y [61].

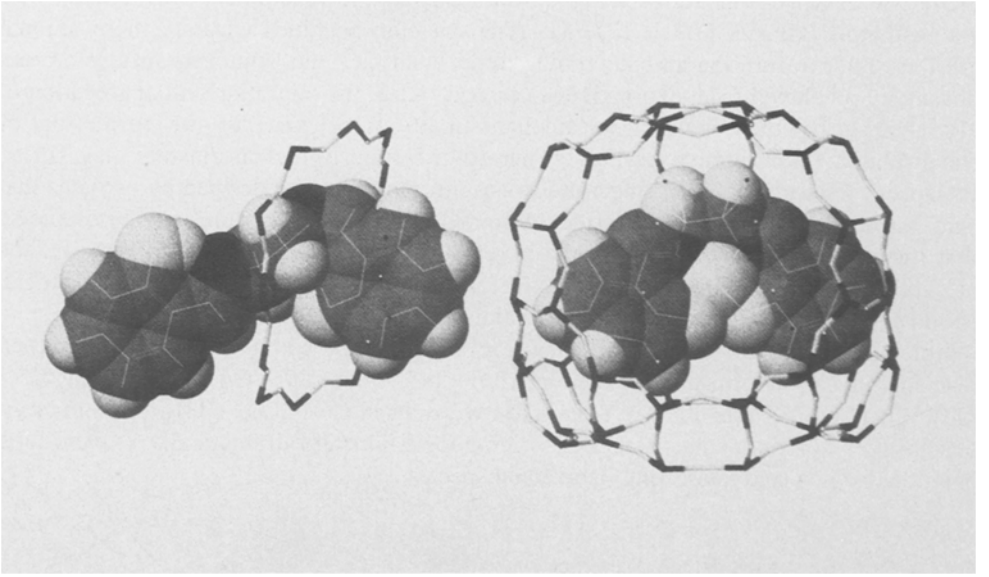

Figure 4. The flexible ligand SALEN is depicted diffusing through a 12-ring to form an FeSALEN complex in a Na-Y supercage.

The flexible ligand method requires a ligand(s) of such dimensions that intrazeolite complexation precludes diffusion back out of the zeolite. This places severe limitations on the number and type of ligands that might be employed. Additionally, the intrazeolite complexation must occur from the outer parts of the crystal to the inner parts. One would anticipate a heterogeneous distribution of complexes as a consequence of pore blockage. Nevertheless, this approach is probably the easiest in practice.

2.3 TEMPLATE SYNTHESIS METHOD

The template synthesis method involves the diffusion of ligand precursors into the zeolite pores where they assemble around an intrazeolite metal ion that acts as a template. This approach is typified by the synthesis of intrazeolite phthalocyanine complexes. The large pore zeolites X, Y, and the aluminum phosphate VPI-5 modified with metal ions, metallocenes (Cp_2Ni, Cp_2Ru, Cp_2Fe, $CpMn(CO)_3$) and metal carbonyl complexes ($Ni(CO)_4$, $Fe(CO)_5$, $Fe_2(CO)_9$, $Co_2(CO)_8$, $Os_3(CO)_{12}$) have been reacted with dicyanobenzene (DCB) to form the intrazeolite MPc complexes. Figure 5 illustrates how 4 DCB molecules would have to approach a FAU type supercage containing an $Fe(CO)_5$ molecule to form the FePc guest complex. The template synthesis of zeolite-encapsulated phthalocyanine complexes of Mn [23,32,42,51], Fe [3,4,21-25,33,47-49,51],

Co [6-18,23,33,35,36,43,47-49,51], Ni [6-10,12,13,15-17,36,38,47-49,51], Cu [6,7,9,10,12-17,30,33,36], Ru [23,36,37,47-49,51], Rh [31], Os [43,47-49], and Ti [51] as well as Li_2Pc and H_2Pc [51] have been reported. The synthesis generally involves heating an intimate mixture of partially dehydrated zeolite with an excess of DCB in a bomb reactor between 150 and 350° C. There has been one report of a solvent mediated reaction at 180° C which appears to lower the reaction temperature [23]. The condensation of four DCB molecules around a metal ion to form a phthalocyanine requires two reducing equivalents, the source of which is the subject of much debate. These electrons may originate from water or the metal ions in the case of the organometallic precursors. This is consistent with the fact that intrazeolite MPc complexes form most easily with zero valent metal carbonyls, followed by metallocenes and metal ions. Better results for MPc formation in ion-exchanged zeolites are obtained when the zeolite is only partially dehydrated.

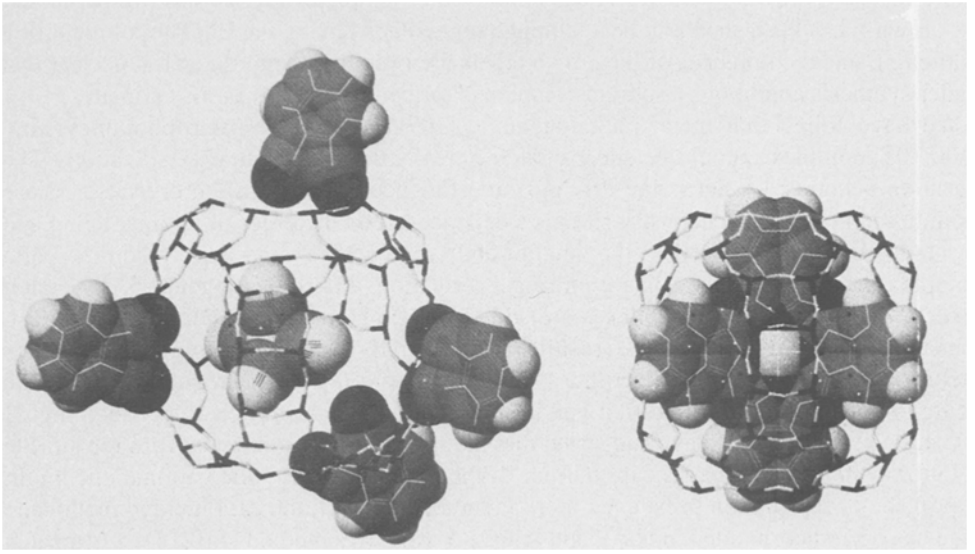

Figure 5. Dicyanobenzene molecules are depicted diffusing into an $Fe(CO)_5$ modified Na-Y supercage to form the encapsulated FePc complex.

Several MPc derivatives have been encapsulated in X and Y type zeolites including perhalogenated phthalocyanine complexes [100,101], *t*-butylphthalocyanines [26,27], and nitrophthalocyanines [51]. There have also been claims of Co-porphyrin [54], Fe- and Mn- tetramethylporphyrin complexes [51,53], as well as tetraphenylporphyrin complexes [23] encapsulated in Na-Y. The porphyrin template synthesis usually requires two reagents, pyrrole and either formaldehyde, acetaldehyde, or benzaldehyde.

2.4 ZEOLITE SYNTHESIS METHOD

The limitations and disadvantages associated with the flexible ligand and template synthesis methods for encapsulating metal complexes in zeolites encouraged us to explore the possibility of crystallizing a zeolite around a metal complex, i.e., build the bottle around the ship. This would afford the advantage of encapsulating a well-defined intrazeolite complex without contamination from free ligand as well as uncomplexed and partially complexed metal ions. There were some early efforts that employed simple chelate complexes such as bis(ethylenediamine)cobalt(II) during zeolite synthesis [102,103]. Unfortunately, these complexes are not stable during zeolite synthesis and may lead to partially exchanged or occluded metal. There have been claims of ZSM-5 and mordenite being synthesized in the presence of MPc complexes [104,105]. However, the 13 Å diameter of the Pc ligand far exceeds the pore dimensions of these zeolites. More recently, crown ethers have been employed as templates for zeolites. In particular, 18-crown-6 has been shown to be a template for zeolites having the EMT topology [106]. Although, metal complexes of the crown ethers are introduced into the gel, it is clear that under synthesis conditions a sodium complex is formed which acts as the template.

We have found that metal phthalocyanine [107-109] and perfluorophthalocyanine [100,101] complexes could be encapsulated in Na-X during zeolite crystallization. The question becomes - what is the driving force for incorporation in the crystals? Close examination of the gel chemistry reveals a dependence on the order of mixing, aging and crystallization time as well as the amount and type of MPc complex. When the MPc complex is mixed with the silica prior to gel formation, a fairly homogeneous dispersion results. However, if the complexes are added to the aluminate or aluminosilicate gels, then a heterogeneous mixture results and virtually no metal complex becomes incorporated in the resulting zeolites. A normal Na-X synthesis requires little or no aging, whereas the MPc modified gels may require aging overnight to produce highly crystalline zeolites. We have suggested that the metal complex interacts with the silicate solution which encourages encapsulation. If the metal complex were cationic one might expect the encapsulation to be even more favorable. In fact, the cationic dye methylene blue has been incorporated in Na-Y and $AlPO_4$-5 using this method [110,111]. It appears that the zeolite synthesis method is a viable approach to preparing ship-in-a-bottle complexes.

Na-X does not require a template so it is not clear what, if any, structure-directing properties the MPc complexes might have. More promising results have been obtained with bis(cyclopentadienyl)cobalt(III) ion, Cp_2Co^+, where ZSM-51 [112], nonasil [63,64], and $AlPO_4$-5 [113] have been crystallized in the presence of this complex. All of these molecular sieves require a structure directing agent. Therefore, cobalticinium ion acts as a template. The zeolite ZSM-51 and the all silica nonasil both have the NON topology [70] which belongs to a family of structural types known as the clathrasils. These molecular sieves are characterized by the complete entrapment of the template during crystallization. The nature of the anion for these syntheses is also important. For example, Cp_2CoPF_6 was claimed as a template for ZSM-51 [112], while we found this

complex resulted in only amorphous materials for the nonasil synthesis. Cp_2CoOH, on the other hand, produced highly crystalline nonasil in both hydroxide and fluoride media after only a few days, while the organic templates typically require several weeks. The encapsulation of Cp_2Co^+ during synthesis resulted in nearly one complex per $[5^86^{12}]$ cage (see Chapter 1, Table 3b, p 8 for details regarding this nomenclature), the only cavity large enough to accommodate the complex. This ellipsoidal cavity, shown in Figure 6, is a 20-hedron cage accessible only through six-membered rings. The Cp_2Co^+ complex easily fits in this cage and appears to have a similar shape. In contrast to the NON cage structure, $AlPO_4$-5 has a one-dimensional channel system which easily accommodates the Cp_2Co^+ complex (Figure 6) but structure-shape relationships are less obvious. Rigid templates such as cobalticinium ion and derivatives may provide information on effects of template symmetry during the synthesis process as well as assist in the rational design of new materials.

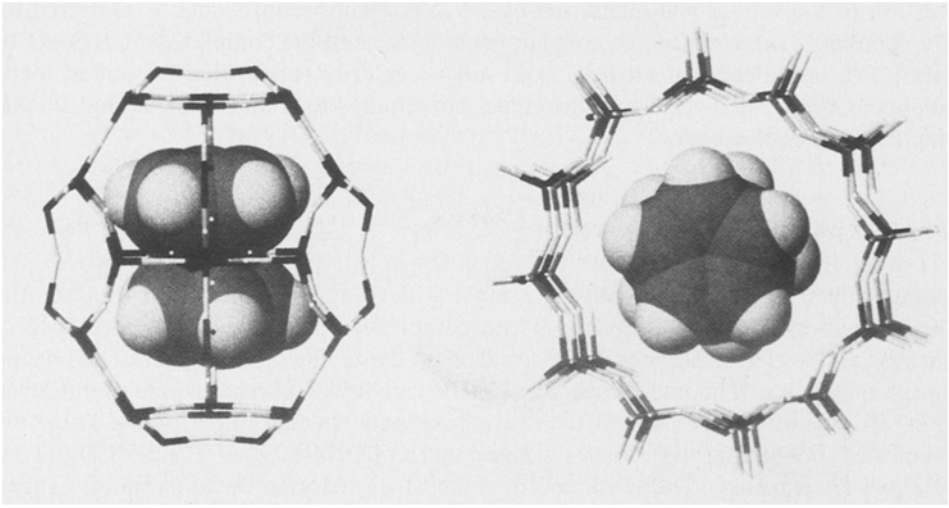

Figure 6. Bis(cyclopentadienyl)cobalt(III) ion is depicted in the nonasil $[5^86^{12}]$ cage (left) and inside a channel of $AlPO_4$-5 (right).

3. Characterization of Intrazeolite Complexes

The characterization of zeolite encapsulated metal complexes is quite difficult and generally requires a battery of techniques in order to convincingly argue for the intrazeolite location of the metal complexes. The first step in this procedure is to remove surface species by Soxhlet extraction with a series of solvents and/or vacuum sublimation. One has to be particularly careful with metal complexes such as the metallophthalocyanines, that strongly adsorb to the metal oxide surface. We have found

that in the case of some zeolites modified with MPc complexes that even after solvent extraction and sublimation some residual metal complex could be removed electrochemically. When a negative potential is applied to freshly prepared zeolite encapsulated MPc complex/graphite composite electrodes, a small amount of reduced metal complex is released from the surface as evidenced by a faint blue color in the electrolyte solution. With subsequent cycles and fresh solvent, there was no further evidence of surface MPc species. This is not the case with zeolites modified with MSALEN complexes where solvent extraction is sufficient to remove surface species. Even though the outer crystal surface area of most zeolites may be several orders of magnitude less than the internal surface area, it is clear that one cannot completely rule out the possibility that there are some complexes adsorbed on the outer surface or partially occluded in mesopores. Therefore, zeolites with very low loadings of metal complex should be considered carefully. In addition to traditional elemental analyses, encapsulated metal complexes such as the phthalocyanines may be recovered after digestion of the zeolite and quantified by UV-Vis spectroscopy. This is preferred for MPc complexes prepared by the template method because the complexation may not be quantitative and elemental analysis does not necessarily reflect the amount of metal complex. Otherwise, a variety of techniques are required to characterize the intrazeolite complexes as detailed below.

3.1 VIBRATIONAL SPECTROSCOPY

Infrared spectroscopy is probably the most widely applied analytical tool for the characterization of zeolite ship-in-a-bottle complexes. Either diffuse reflectance or transmission IR spectra can provide information on the zeolite lattice as well as the nature of guest molecules. The mid-IR spectra of metal carbonyl clusters are quite useful given the sensitivity of the CO ligand to its environment. In fact, most of the structural evidence of such intrazeolite clusters is based on CO [72,74-80,85-97] and ^{13}CO [92,94] stretching frequencies. The weak coordination of a supported metal carbonyl oxygen with the zeolite host (eqn. 1) may affect the stability and reactivity of encapsulated clusters.

$$M\text{-}C{\equiv}O\cdots\cdots Na^{+}Z^{-} \qquad (1)$$

A shift for both bridging and terminal carbonyl IR stretching frequencies relative to the free clusters, is consistent with this type of interaction. Such shifts have been noted for several encapsulated metal carbonyl clusters [72,78,79,85,88,89,91,97,98]. The zeolite lattice effects are also influenced by water. Zeolite encapsulated $Ir_4(CO)_{12}$ upon dehydration exhibits bridging carbonyl bands in the IR which were interpreted as a consequence of removing the protective sheath of water between the cluster and the electrostatics of the cage [76].

The mid-IR spectroscopic results for intrazeolite MPc [25,28,31,33,45,47-49,51],

substituted MPc [26,27,100,101] and MSALEN [55,56,58,61] complexes have been reported. The various T-O vibrational modes associated with the zeolite dominate most of the region between 1150-450 cm^{-1}, however, at reasonable loadings, the complexes can be detected. The bands associated with C=N and C=C stretching modes for the Pc ligand are easily observed and may show a slight shift to lower wavenumbers inside the zeolite. Kimura et al. have interpreted this shift as a result of ligand distortion in the supercage [28]. However, intrazeolite MPc complexes prepared by the template method may contain free Pc ligand which could account for lower frequency bands [51]. The complexation of SALEN should result in a blue shift of a strong C=C stretch at 1504 cm^{-1}. Other bands not associated with free ligand or complex have been observed [56,61] and may be the result of coordination modes other than tetradentate.

The resonance Raman spectra for Li_2Pc, TiPc and FePc in Na-Y suggest that the intrazeolite complexes are not distorted from D_{4h} symmetry [51]. Such a distortion might be expected to result in the generation of new bands as well as a loss of others. At this point it is not clear where the anticipated spectral changes would be observed. However, these results are in agreement with NMR results obtained in the same study.

3.2 ELECTRONIC SPECTROSCOPY

Electronic spectra can be useful in evaluating intrazeolite complexation as well as any structural perturbations that might occur as a consequence of encapsulation. The aromatic phthalocyanines are intensely blue and green with extinction coefficients on the order of 10^5. Therefore, the UV-Vis spectra of MPc modified zeolites, even those containing low loadings of MPc, are readily obtained as Nujol mulls or via reflectance techniques. The most intense band for the complexes is a Pc based $\pi \rightarrow \pi^*$ transition known as the Q band which is typically in the range of 600-900 nm. MPc complexes encapsulated in FAU type zeolites generally exhibit a Q band that is red-shifted relative to the free or surface physisorbed complex. Shultz-Ekloff first observed these spectral changes [35] and Herron later suggested that this arises from distortion of the planar Pc ligand as a result of steric interactions within the supercage [22]. Molecular modeling predicts a saddling of the MPc complex which is in agreement with the fact that the Pc ligand is slightly larger than the 12 Å diameter of the supercage. XPS [14,36,37], EXAFS [25-28], and IR [28] results might be interpreted as consistent with a deformation of the ligand from planarity. However, Raman and NMR results [51] suggest there is no distortion. If the intrazeolite MPc complexes are not distorted, then a bathochromic shift for the Q band might arise from zeolite solvent effects. FePc in sulfuric acid exhibits an ~100 nm red-shift of the Q band relative to organic solvents which is attributed to protonation of the peripheral nitrogens. It has been suggested that intrazeolite phthalocyanines might be protonated [122]. Evidence for protonated intrazeolite Pc species has been reported by Parton et al. [45]. Additionally, XPS results could be interpreted as a result of protonated nitrogens [36,37]. It is also quite amazing that Na-X can be synthesized around a MPc complex that has to be distorted. Nevertheless, the

saddle structure for a zeolite encapsulated phthalocyanine is possible and probable given the constraints of the supercage. Similarly, the Q band for FePc(t-Bu)$_4$ (19 x 19 Å) prepared in Na-Y [27] is red shifted. Additionally, zeolite encapsulated tetramethylporphyrin complexes exhibit a suppressed Q band which has been interpreted as an effect of ligand distortion in the supercage [53].

The UV-Vis spectra of intrazeolite SALEN complexes are not quite as sensitive to structural perturbations. The bright yellow SALEN ligand exhibits bands at 323 and 409 nm which shift upon complexation. Both Mn(II) and Mn(III)SALEN [55] as well as Rh(III) [56], Pd(II) [58] and Co(II)SALEN [59] have been characterized by UV-Vis spectroscopy.

The color of the intrazeolite Chini-type carbonyl clusters vary with nuclearity such that $[Pt_9(CO)_{18}]^{2-}$ (orange-brown), $[Pt_{12}(CO)_{24}]^{2-}$ (dark green), and $[Pt_{15}(CO)_{30}]^{2-}$ (yellow-green) are readily characterized by their UV-Vis spectra [90-92]. Differences between solution and encapsulated clusters have been noted but not explained. Perhaps the interaction of coordinated CO with the zeolite lattice contributes to these differences, however, this needs to be studied further.

3.3 ELECTRON PARAMAGNETIC RESONANCE/MÖSSBAUER

Both EPR and Mössbauer spectroscopy provide information on the states of iron-based zeolite ship-in-a-bottle complexes [25-28,39-41]. The Mössbauer spectra of Fe(II)Pc encapsulated in Y type zeolites indicate the presence of two types of FePc, one that is reactive with pyridine (py) and one that is not [39-41]. The formation of FePc(py)$_2$ depends on the free volume within the supercage. FePc entrapped in Na-Y, K-Y, and Rb-Y showed a decreasing tendency to react with pyridine as the size of the charge balancing cation was increased [41]. There is very little difference in the isomer shift or quadrupole splitting between intrazeolite and free FePc. In contrast, the Mössbauer spectrum for FePc(t-Bu)$_4$ inside the zeolite is quite different from the free complex and indicates reduced electron density for the encapsulated Fe [26,27]. A temperature dependence study of the Mössbauer absorption area of FePc in Na-Y indicated the results do not follow a Debye approximation suggesting the complexes are well-dispersed [39]. Complimentary EPR experiments indicate the FePc complexes are close enough for the spins to interact [41].

A dioxygen adduct of Na-Y encapsulated CoSALEN has been studied by EPR [2]. The intrazeolite CoSALEN prepared by the flexible ligand method is EPR silent and presumably high-spin Co(II). Exposure to pyridine still does not generate an EPR signal, however, subsequent absorption of oxygen produces a classic EPR spectrum for a Co-O_2 adduct. The signal is axial which indicates the complex is not rotating in the supercage. Additionally, the EPR parameters are quite similar to those obtained in solution such that the intrazeolite complex is probably not distorted.

3.4 NUCLEAR MAGNETIC RESONANCE

There has been only one report of zeolite ship-in-a-bottle complexes being characterized by solid-state NMR [51]. Na-Y encapsulated Li_2Pc, FePc, $Fe(nitro)_4Pc$, and TiPc were studied using cross-polarization magic-angle-spinning ^{13}C-NMR. There are 8 different carbons that can be differentiated by this technique, but only 4 were resolved for the intrazeolite species. One might expect the carbon resonances to shift as the hybridization or aromaticity is altered by distortion of the Pc macrocycle from planarity inside the supercage. However, the peaks observed for zeolite encapsulated TiPc were nearly the same as for the free complex. This would seem to argue against any significant deformation of the intrazeolite Pc ligand. The fact that four signals are well-resolved and have narrow line widths suggests the complexes are fairly symmetric. The FePc in Na-Y was shown to be largely free H_2Pc ligand which again is a consequence of the template method of encapsulation.

The ^7Li-NMR spectra of Na-Y modified with Li_2Pc indicate the surface and entrapped complexes can be resolved. The signal for the intrazeolite complex was shifted ~1.8 ppm upfield from the surface complex which was attributed to the effects of the electrostatic field inside the zeolite [51].

Zeolites containing paramagnetic metal ions have been shown to be effective contrast agents for magnetic resonance imaging (MRI) [114]. A diagnostic pharmaceutical for this purpose known as GADOLITE®, which is based on a Gd(III) modified Na-Y zeolite, is currently in clinical trials. As part of this effort, Gd(III) complexes of 8-hydroxyquinoline were prepared in zeolites Na-X and Na-A by the zeolite synthesis method [115]. In the case of the Na-A zeolite, the 4.1 Å apertures to the large cage preclude the 8-hydroxyquinoline ligand from entering. Therefore, the only way to prepare such ship-in-a-bottle species is to crystallize the zeolite around the complexes. A measure of potential in vivo efficacy as an MRI contrast agent is the relaxivity which represents the relationship between water proton T_1 shortening and gadolinium concentration. Preliminary results suggest the intrazeolite complexes exhibit higher relaxivities than the ion-exchanged zeolites.

3.5 ELECTROCHEMISTRY

There is a well-established effort to include zeolites in the design of new electrocatalytic surfaces as evidenced from recent reviews [116,117]. The application of cyclic voltammetry to characterize intrazeolite metal complexes has also proven to be quite useful. Both intrazeolite metal SALEN [60-62] and phthalocyanine [50,62] as well as perfluorophthalocyanine [62,100,101] complexes have been characterized electrochemically.

For the zeolite ship-in-a-bottle complexes, electron transfer must occur inside the zeolite, presumably by an extended electron-hopping mechanism [118]. Therefore, communication between zeolite cavities depends on the complex loading. The outermost

supercages of the zeolite crystals in contact with graphite will be redox accessible. However, the presence of vacant supercages hinders the electron transfer process between complexes in the bulk. Additionally, occupied cages may prevent solvent and electrolyte from reaching inner crystal redox sites. As a result, only a few percent of the encapsulated metal complexes are electroactive. The addition of a surface mediator, such as a metal complex too large to enter the zeolite, can improve the electrochemical response of the entrapped complexes [118]. However, electrochemical access to all of the encapsulated complexes remains a challenge. For those intrazeolite metal complexes that are redox accessible, the possibility exists for developing new types of electrocatalysts. The catalytic reduction of alkyl halides was demonstrated for CoSALEN in Na-Y [60] and the electrochemical formation of MnSALEN superoxo and oxo species [61] presents an opportunity for exploring oxidation electrocatalysis.

3.6 X-RAY METHODS

X-Ray powder diffraction is certainly an indispensable technique for the zeolite synthesis method where phase identification and purity are critical. XRD also provides valuable information on crystallinity as well as any change in unit cell parameters that might arise from the in situ generation of intrazeolite ship-in-a-bottle complexes. Variations in peak intensities resulting from a redistribution of charge balancing cations after inclusion of cationic complexes in the supercage have been noted. However, for the most part, ship-in-a-bottle complexes are neutral. Intrazeolite MPc complexes, including the perfluorinated analogs, have never shown an expansion of an X or Y zeolite unit cell in spite of the fact that the complex has a tight fit inside the supercage [22,31,33,35,45, 51,100,101]. Zeolite crystallinity is largely preserved after the encapsulation of MPc complexes by the template method. Complexes prepared from ion-exchanged zeolites might be more susceptible to dealumination as the formation of protons is likely. The preparation of RhPc complexes in Y or X zeolites results in a loss of crystallinity, however, this system also involves partial reduction of the Rh(III) [31]. The zeolite crystallinity was reported to be intact after entrapped MnSALEN was prepared by the flexible ligand method [55]. Na-Y was also found to be unaffected by the generation of intrazeolite osmium carbonyl clusters [87].

The intrazeolite carbonyl clusters are more often characterized by extended X-ray absorption fine structure spectroscopy (EXAFS). This technique provides valuable information on the type and number of atoms as well as the distance between them. Unfortunately, access to the required synchrotron radiation may be limited. X-Ray absorption near edge spectra (XANES) are often obtained with EXAFS and generally are used to evaluate oxidation states. EXAFS spectroscopy has provided evidence of $Ir_4(CO)_{12}$ [89,94], $[Ir_6(CO)_{15}]^{2-}$ [89], $Rh_6(CO)_{16}$ [72,78], $[Ni(CO)_4]_2$ [97], and $[Pt_3(CO)_6]_n^{2-}$ [91,92,94]. Both the Rh_6 and Chini-type clusters appear to interact with the zeolite framework - with the latter complexes possibly being distorted. The formation of Na-Y encapsulated FePc was confirmed by XANES and EXAFS [25,28]. The Fe-N

distance was determined to be slightly longer than for the free complex which is consistent with distortion of the complex in the supercage. Similarly, Na-Y modified with Fe(*t*-butyl)$_4$Pc exhibited a longer Fe-N distance and a lower coordination number for Fe (3.6) [26,27]. These results do not confirm encapsulation but agree with other spectroscopic results. For a more detailed description of X-ray techniques used in characterization see Chapter 3 by Parise in this volume.

3.7 SURFACE AREA/ADSORPTION EXPERIMENTS

Since zeolite surface area is largely internal, the inclusion of guest molecules should dramatically reduce the absorption capacity of such molecular sieves. The BET surface area of X and Y zeolites containing MPc complexes (M=Mn,Fe,Co,Cu) [32,33] and Co porphyrin [54] are typically less than 100 m^2g^{-1} which is a reduction of at least 600 m^2g^{-1}. Interestingly, the nitrogen absorption capacity of Na-X with entrapped CoPc was reduced by only half [35]. This indicates very little pore blockage at the surface and may attest to the distribution of complexes. The absorption capacity for water in X and Y zeolites containing FePc was reported to be reduced [20]. The absorption results for O_2 at -78 and -196° C by zeolites modified with MPc complexes (M=Co,Cu,Ni) indicated a high dispersion of complexes [7,9]. Pre-absorption of pyridine by these zeolites reduces O_2 absorption in the order NiPc>CoPc>CuPc [12]. Probe molecules such as bulky phosphines have not been applied to the intrazeolite clusters, MPc, or MSALEN complexes but have shown promise in discriminating surface versus internal species, as well as generating ship-in-a-bottle complexes [1,97].

3.8 THERMAL METHODS

Differential Scanning Calorimetry (DSC) has been used to study the energetics of intrazeolite MPc formation by the template synthesis method [29,30]. In the case of CuPc, it was found that the exotherm for CuPc formation occurs at increasing temperature in the order $CuCl_2$<CuNa-Y<CuNa-X<CuNa-A (surface only). The lower peak temperature for CuNa-Y is attributed to the higher mobility of Cu^{2+} in the Y zeolite. The amount of intrazeolite CuPc complex formed in Na-Y increased with both increasing copper loading as well as pressure. At low pressure and high copper loadings, the exotherms for CuPc formation both inside and outside the zeolite can be resolved, where the intrazeolite complex is formed at higher temperatures.

Differential Thermal Analysis (DTA) [33,35] and Thermogravimetric Analysis (TGA) [32,51] have been used to characterize intrazeolite MPc complexes prepared by the template method. The amount of intrazeolite MPc can be estimated from the weight loss and is generally more accurate than the spectrophotometric analysis after zeolite digestion. In the case of iron(II) phthalocyanine and tetranitrophthalocyanine complexes in Na-Y, several exotherms are observed during the decomposition which have been

ascribed to free ligand and organic residues [51]. The encapsulated complexes appear more thermally stable than the free complexes. These results are in contrast with those observed by Gudkov et al. [14,15] where zeolite Y encapsulated CoPc, CuPc and NiPc were deemed less stable than the free complexes. This difference was ascribed to the distortion of the Pc ligand in the supercage.

3.9 SURFACE TECHNIQUES

X-Ray photoelectron spectroscopy (XPS) has been applied to the characterization of intrazeolite MPc [14,18,22,33,36,37,47-49] and MSALEN [2,56,59] complexes. XPS can provide information on the relative concentration of elements and oxidation states in the first ~50 Å of the zeolite which may actually reflect less than 1% of the crystal. Nevertheless, shifts in binding energies for both the intrazeolite metals and nitrogen in SALEN or phthalocyanines indicate complexation. Shpiro et al. noted two types of nitrogens for Na-Y encapsulated Ni, Cu, Co, and RuPc [14,36,37]. This was interpreted as either the result of Pc ligand distortion or strong interactions with the zeolite lattice. A close match between surface concentrations, estimated from metal/Si or metal/Al ratios, and bulk elemental analyses has been used as evidence for a homogeneous distribution of intrazeolite complexes. A higher concentration of metal at the surface does not necessarily imply extrazeolite complexes since ions and molecules may migrate close to the surface as a consequence of the thermal treatment associated with the flexible ligand or template syntheses.

Scanning and transmission electron microscopy (SEM or TEM) provides evidence for metal complex or metal oxide depositions on the outer zeolite crystal surface. SEM images of zeolites modified with MPc complexes before and after solvent extraction exhibit significant changes in crystal surface morphology [18,33,35]. For comparative purposes, Meyer et al. prepared a Na-Y covered with a two-dimensional phthalocyanine polymer derived from tetracyanobenzene which showed a uniform but roughened surface [18]. Whereas the solvent extracted MPc/Na-Y samples had smooth, clean surfaces. Zeolite encapsulated Co porphyrin was also studied by SEM with similar results [54]. TEM has provided evidence of uniform dispersions of osmium carbonyl clusters in Y type zeolites [87]. These techniques, in concert with the others described above, provide compelling evidence for the intrazeolite location and distribution of metal complexes.

3.10 COMPUTER MODELING

Molecular modeling is rapidly becoming an indispensable tool for predicting zeolite guest/host interactions as well as corroborating empirical results. Both the phthalocyanine [22,45,51,100,119,120] and SALEN [2,58,61] complexes have been modeled in the FAU supercage. Several important questions have been posed including, are the intrazeolite MPc complexes distorted and is MSALEN truly entrapped? Herron

first reported a zeolite Y encapsulated FePc model where a saddle distortion of <20° from planarity allowed the phenyl rings to poke through the supercage windows without any close van der Waals contacts [22]. Subsequently, Parton et al. calculated the minimum Pc ligand distortion to be 37.27° from planarity using Chem-X software [45]. It was also shown that FePc in the 12.1 Å cylindrical channels of VPI-5 is not distorted if the complex is positioned between two opposite 6-rings. There is no such possibility of steric relief in the 12 Å FAU supercage given the spherical nature of the cavity. The lowest energy configuration of $FeF_{16}Pc$ in Na-Y was found to be distorted 34.5° from planarity using CAChe molecular mechanics and MM2 parameters [100]. The consistency of these calculations in predicting a saddle shape complex argues for the distortion used to explain many spectroscopic results.

CoSALEN and the pyridine adduct were modeled inside Na-Y and shown to be entrapped [2]. However, De Vos et al. claimed that by moving the CoSALEN in small steps (0.2 Å and 3°), the complex could pass through the supercage windows [58]. This was accomplished using Chem-X software and crystallographic parameters for CoSALEN. This calculation does not take into account other absorbed molecules or the lowest energy configuration for encapsulated MSALEN. A possible bidentate SALEN complex with iron at an S_{II} site was also modeled using CAChe software [61]. Since the nature of the ligand coordination appears to vary with the metal ion, it may be appropriate to refer to intrazeolite SALEN complexes as sterically hindered.

4. Reactivity

A number of reviews have appeared which specifically address catalytic advances in the area of zeolite guest/host chemistry, especially ship-in-a-bottle complexes [120-127]. The largest effort is directed towards the development of oxidation catalysts, although, a number of new applications are beginning to emerge. In addition to the potential for new catalyst development, reactivity studies can provide convincing evidence for the encapsulation of metal complexes.

4.1 DIOXYGEN BINDING

Some of the major challenges in the development of a commercially viable oxygen carrier include capacity and reversibility. A target capacity of 10 cc O_2/g of carrier is amenable to the high surface area zeolites modified with metal complexes. Additionally, the zeolite ship-in-a-bottle complexes are effectively site-isolated which precludes formation of peroxo-bridged dimers that could occur on conventional supports or in solution. Zeolite Na-Y encapsulated CoSALEN which is EPR silent and presumably high-spin Co(II), is unreactive towards O_2. However, intrazeolite CoSALEN readily binds O_2 after the complex is exposed to pyridine [2,59]. A negative cooperativity was deduced from Hill plots which was interpreted as the ability of the zeolite to maintain an

O_2 pressure within the pores that was effectively greater than the external pressure [2]. This system may actually be more complicated since electrochemical studies have shown it is possible to have at least two types of intrazeolite CoSALEN complexes with only one that binds pyridine [60].

4.2 OXIDATION CATALYSIS

Herron et al. first reported the oxidation of alkanes by iodosylbenzene, catalyzed by FePc encapsulated in zeolites Na-X and Na-Y [3]. Substrate selectivity was reported where, in a competitive experiment, cyclohexane was preferentially oxidized over cyclododecane. The oxidation of n-octane favored the 2-position near the end of the molecule which is presumably the result of orientation effects in the zeolite. Norbornane was oxidized to norborneol with an exo:endo ratio of 6 compared with the ratio of 9 observed with the homogeneous catalyst. Na-Y encapsulated FePc catalyzed methylcyclohexane oxidation with a turnover number of 5.6 and a yield of *trans/cis* alcohols at the 4 position in a 2:1 ratio whereas the free FePc complex gave a 1.1:1 mixture and 1.1 turnovers. It was later shown that the selectivity could be further modified by changing the charge balancing cation of the zeolite [22]. Although the activity of intrazeolite FePc was greater than the free complex, it was still rather poor and this was attributed to pore blockage by iodoxybenzene [3]. Subsequently, Parton et al. reported that using *t*-butylhydroperoxide and Na-Y zeolites containing 1 FePc complex per 77 supercages for the oxidation of alkanes resulted in turnovers as high as 6000 [45,46]. Not only was the lower FePc loading deemed significant in the prevention of pore blockage, but the original source of iron, ferrocene, was also important in reducing the amount of uncomplexed iron. The encapsulated FePc eventually deactivates, presumably from ligand degradation. In fact, the peroxide must be slowly added because the catalyst can be easily bleached with excess oxidant. Interestingly, FePc occluded inside VPI-5 appears more stable than the FAU zeolite analogs, with no signs of deactivation even after 2000 turnovers [46]. There are two major differences between these ship-in-a-bottle systems. Firstly, inside VPI-5 the complex is predicted to be planar and secondly, the one-dimensional channels of VPI-5 may limit activity to the ends of the pores.

Both MnPc [32,51] and MnSALEN [55] encapsulated in Na-Y have been reported to catalyze the oxidation of alkenes using iodosylbenzene. In contrast to FePc, the activity of intrazeolite MnPc is considerably lower than for the free complex but the selectivity is altered [32]. For example, the conversion of 1-undecene is greater than for 2-octene which is the opposite of that obtained with the free complex. Similarly, the conversion of *trans*-2-octene is greater than *cis*-2-octene which again is opposite from the homogeneous catalyst. Na-Y encapsulated MnSALEN also exhibited much lower activity than the free complex which was attributed to substrate diffusion and competition with solvent oxidation. However, shape selectivity was observed with the order of reactivity, cyclohexene>styrene>*trans*-stilbene. This is in contrast to free MnSALEN which exhibits the opposite selectivity. Substitution of the Pc ligand periphery with four nitro

groups enhances the catalytic activity of the Mn and Fe complexes [51]. This is believed to be the result of their electron withdrawing properties. A perfluorinated phthalocyanine complex of iron, which we anticipate will exhibit further enhanced catalytic activity and oxidative stability, has been encapsulated and reactivity studies are in progress [100].

There are relatively few examples of O_2 oxidations catalyzed by zeolite-encapsulated MPc complexes. Na-X encapsulated CoPc was found to facilitate the oxidation of propene to formaldehyde and acetaldehyde, while the free complex was unreactive and Co-Y produced acetone [35]. The oxidation of methane at 375° C catalyzed by Na-Y encapsulated Co, Fe, Mn and Ru phthalocyanines as well as tetraphenylporphyrin complexes produced primarily CO_2 and H_2O [23]. The intrazeolite RuPc, CoTPP, and MnTPP produced some methanol. The oxidation of cumene catalyzed by FePc [21] and cysteine by CoPc [11] in Na-Y have also been reported.

Zeolite-encapsulated MPc complexes are beginning to attract interest as eco-catalysts. Romanovsky et al. have studied the oxidation of CO and the reduction of NO [7,12,47-49]. CO can be converted to CO_2 over the temperature range -78 to 60° C. At room temperature, CO_3^{2-} forms and poisons the catalyst. However, pre-absorption of pyridine prevents formation of carbonate over these catalysts. NO was reduced by both CO and H_2 over MPc (M=Co,Fe,Ni,Ru,Os) complexes entrapped in Na-Y zeolites between 200 and 300° C. In all cases, CoPc/Na-Y was the most active, producing primarily NH_3 during H_2 reduction and N_2O during CO reduction of the NO. Zeolite-encapsulated $[Pt_3(CO)_6]_n^{2-}$ clusters have also been shown to be effective catalysts for NO reduction by CO [91,92].

4.3 HYDROGENATION CATALYSIS

Palladium(II)SALEN is an efficient catalyst for the room temperature hydrogenation of olefins but poorly selective [128]. Encapsulation of the PdSALEN complex in zeolites Na-X or Na-Y dramatically enhances the substrate selectivity. For example, a mixture of cyclohexene and 1-hexene are converted to nearly equal amounts of cyclohexane and n-hexane by the free PdSALEN complex whereas the zeolite encapsulated PdSALEN hydrogenates only the terminal olefin in the same mixture [57]. For a mixture of cyclooctadiene and 1-octene, the hydrogenation of 1-octene was suppressed [58]. It was also shown in this study that the zeolite encapsulated PdSALEN was more selective for the hydrogenation of cyclooctadiene to cyclooctene than Pd on carbon or PdY. The results for hydrogenation of the diene and mono olefins in these two studies require further study; however, at this point it is clear that the complexation of intrazeolite Pd(II) imparts reactivity not observed in solution or with supported Pd.

The catalytic hydrogenation of toluene to methylcyclohexane in the presence of iron(II) phthalocyanine encapsulated in Na-Y has been reported [34]. Benzene was unreactive under the same conditions so it was proposed that the methyl group of toluene interacts with the zeolite lattice favoring reaction. FePc/Na-Y was reported to be unreactive towards butadiene hydrogenation [28]. However, treatment of the intrazeolite FePc with

sodium naphthalide induces catalytic activity. At low conversions, higher selectivity was observed towards *trans*-2-butene compared with the extra zeolite $(Na^+)_4(FePc^{4-})$ donor-acceptor complex.

The hydrogenation of CO catalyzed by several intrazeolite carbonyl clusters has been reported [72,86,87,89]. The encapsulated $Ir_4(CO)_{12}$ [89], $[Ir_6(CO)_{15}]^{2-}$ [89], and $HOs_3(CO)_{11}^-$ [86,87] produce hydrocarbons but in a non-Schultz-Flory distribution where the selectivity is towards alkene rich C_2-C_4 molecules.

4.4 OTHER REACTIONS

There are a variety of reactions where the metal carbonyl clusters are either precursors to metal particles or the clusters are simply implicated in the mechanism [71]. There is proportionately less information available on intact intrazeolite carbonyl clusters involved in catalysis. The water gas shift reaction has been reported to be catalyzed by $HFe_3(CO)_{11}^-$ [85] and $[Pt_3(CO)_6]_n^{2-}$ (n=3,4) [129] in Na-Y. The iron cluster catalyst exhibited high activity at low temperatures (60-180° C) and atmospheric pressure. The intrazeolite Chini clusters, which were also quite active at low temperatures (50-150° C), displayed enhanced activity (38 times higher) during illumination from a Xe lamp.

Zeolite encapsulated metal phthalocyanines have been reported to be effective catalysts for the dehydrogenation of cyclohexane [7,15] and isopropanol [7,8]. It was noted that pre-absorption of aromatics such as pyridine enhanced the activity of intrazeolite NiPc and CoPc but not that of CuPc. The conversion of cyclohexene oxide catalyzed by zeolite encapsulated CuPc was found to be nearly 100% selective for cyclohexadiene [10]. Finally, the conversion of butylmercaptan to butylenes, dibutylsulfide, and hydrogen sulfide over Na-Y zeolites containing various metal phthalocyanines was reported [16] and more recently, Na-X encapsulated CoPc was shown to be an efficient catalyst for the oxidation of mercaptans to disulfides [44].

5. Future Trends

It should be apparent that a large effort has been directed towards the preparation and characterization of zeolite ship-in-a-bottle complexes. The synthesis of molecular sieves around metal complexes is probably the most versatile strategy discussed because there is no predetermined size restrictions on the complex. Since the complexes are well-defined before encapsulation, the characterization of the intrazeolite species should be easier. Additionally, there are no limitations as to the pore dimensions or structural composition of potential host molecular sieves. Moreover, the possible structure directing properties of a metal complex presents exciting opportunities for the generation of new molecular sieves.

The bulk of this review has involved the modification of synthetic faujasite type zeolites, partly because of the pore structure. The diffusional limitations of the X or Y

zeolite containing metal complexes casts some doubt as to the commercial viability of such catalysts. However, there are many new porous materials such as MCM-41 [130] or cloverite [131] that would be amenable to the encapsulation methods outlined above. One could imagine that structural and compositional variance might impart new and interesting properties to a ship-in-a-bottle complex. In addition to the many catalytic transformations that will undoubtedly be elucidated in the near future, we expect new directions in areas ranging from pharmaceuticals to materials chemistry will be forthcoming.

References

1. N. Herron, G. D. Stucky, and C. A. Tolman, *Inorg. Chim. Acta*, **100**, 135 (1985).
2. N. Herron, *Inorg. Chem.*, **25**, 4714 (1986).
3. N. Herron, C. A. Tolman, and G. D. Stucky, *J. Chem. Soc., Chem. Commun.*, 1521 (1986).
4. R. Parton, D. De Vos, and P. A. Jacobs, in *Proceedings of the NATO Advanced Study Institute on Zeolite Microporous Solids: Synthesis, Structure and Reactivity*, E. G. Derouane, F. Lemos, C. Naccache, and F. R. Ribeiro (Eds), Kluwer, Dordrecht, pp 555 - 578 (1992).
5. N. Herron, *Chemtech,* **19**, 542 (1989).
6. V. Yu. Zakharov and B. V. Romanovsky, *Vestn. Mosk. Univ., Ser. Khim.*, **18**, 142 (1977) [Eng. Trans. in *Sov. Mosc. Univ. Bull.*, **32**, 16 (1977)].
7. B. V. Romanovsky, R. E. Mardaleishvili, V. Yu Zakharov, and O. M. Zakharova, *Vestn. Mosk. Univ., Ser. 2: Khim.*, **18**, 232 (1977).
8. V. Yu. Zakharov and B. V. Romanovsky, *Vestn. Mosk. Univ., Ser. 2: Khim.*, **18**, 348 (1977).
9. V. Yu. Zakharov, O. M. Zakharova, B. V. Romanovsky, and R. E. Mardaleishvili, *React. Kinet. Catal. Lett.*, **6**, 133 (1977).
10. M. V. Gusenkov, V. Yu. Zakharov, and B. V. Romanovsky, *Neftekhimiya*, **18**, 105 (1978).
11. O. M. Zakharova and B. V. Romanovsky, *Vestn. Mosk. Univ., Ser. 2: Khim.*, **20**, 284 (1979).
12. B. V. Romanovsky, O. M. Zakharova, and V. Yu. Zakharov, *Vestn. Mosk. Univ., Ser. 2: Khim.*, **20**, 43 (1979).
13. V. Yu. Zakharov and B. V. Romanovsky, *Vestn. Mosk. Univ., Ser. 2: Khim.*, **20**, 78 (1979).
14. S. V. Gudkov, E. S. Shpiro, and B. V. Romanovsky, *Izv. Akad. Nauk. SSSR, Ser. Khim.*, 2448 (1980).
15. S. V. Gudkov, B. V. Romanovsky, E. S. Shpiro, G. V. Antoshin, and Kh. M. Minachev, *VINITI Deposited Doc.,* 2472 (1980), [CA **95**:61069n (1981)].
16. O. M. Zakharova and B. V. Romanovsky, *Neftekhimiya*, **21**, 924 (1981).

17. B. V. Romanovsky, in *Proceedings of the 8th International Congress on Catalysis,* Verlag Chemie, Weinheim, p 657 (1984).
18. G. Meyer, D. Wohrle, D. Mohl, and G. Schultz-Ekloff, *Zeolites*, **4**, 30 (1984).
19. A. N. Zakharov and B. V. Romanovsky, *J. Inclus. Phenom.*, **3**, 389 (1985).
20. N. Herron, G. D. Stucky, and C. A. Tolman, *J. Chem. Soc., Chem. Commun.*, 1521, (1986).
21. T. V. Korol'kova and B. V. Romanovsky, *Neftekhimiya*, **26**, 546 (1986).
22. N. Herron, *J. Coord. Chem.*, **19**, 25 (1988).
23. Y. W. Chan and R. B. Wislon, *Preprint Papers - ACS, Div. Fuel Chem.*, **33**, 453 (1988).
24. T. Kimura, A. Fukuoka, and M. Ichikawa, *Shokubai*, **31,** 357 (1988).
25. T. Kimura, A. Fukuoka, and M. Ichikawa, *62th CATSJ Meeting Abstr.: No. 1D203*, **30**, 444 (1988).
26. T. Kimura, A. Fukuoka, and M. Ichikawa, *64th CATSJ Meeting Abstr.: No. 1A09*, **31**, 357 (1989).
27. M. Ichikawa, T. Kimura, and A. Fukuoka, *Stud. Surf. Sci. Catal.*, **60**, 335 (1991).
28. T. Kimura, A. Fukuoka, and M. Ichikawa, *Catal. Lett.*, **4**, 279 (1990).
29. K. J. Balkus, Jr. and J. P. Ferraris, *J. Phys. Chem.*, **94**, 8019 (1990).
30. J. P. Ferraris, K. J. Balkus, Jr., and A. Schade, *J. Inclus. Phenom. Molec. Recog. Chem.*, **14**, 163 (1992).
31. K. J. Balkus, Jr., A. A. Welch, and B. E. Gnade, *J. Inclus. Phenom. Molec. Recog. Chem.,* **10**, 141 (1991).
32. Z. Jiang and Z. Xi, *Fenzi Cuihua*, **6**, 467 (1992), [CA **118**: 212554 (1992)].
33. W. Zhang, X. Ye, and Y. Wu, *Fenzi Cuihua*, **5**, 168 (1991), [CA **115**: 143584x (1991)]
34. A. N. Zakharov, *Mendeleev Commun.*, 80 (1991).
35. H. Diegruber, P. J. Plath, and G. Schultz-Ekloff, *J. Mol. Catal.*, **24**, 115 (1984).
36. E. S. Shpiro, G. V. Antoshin, O. P. Tkachenko, S. V. Gudkov, B. V. Romanovsky, and Kh. M. Minachev, *Stud. Surf. Sci. Catal.,* **18**, 31 (1984).
37. A. G. Gabrielov, A. N. Zakharov, B. V. Romanovsky, O. P. Tkachenko, E. S. Shpiro, and Kh. M. Minachev, *Koord. Khim.*, **14**, 821 (1988).
38. A. G. Gabrielov, A. N. Zakharov, and B. V. Romanovsky, *Koord. Khim.*, **14**, 214 (1988).
39. M. Tanaka, Y. Sakai, T. Tominaga, A. Fukuoka, T. Kimura, and M. Ichikawa *J. Radioanal. Nucl. Chem., Lett.*, **137**, 287 (1989).
40. M. Tanaka, Y. Minai, T. Watanabe, and T. Tominaga, *J. Radioanal. Nucl. Chem., Lett.*, **154**, 197 (1991).
41. M. Tanaka, Y. Minai, T. Watanabe, and T. Tominaga, *J. Radioanal. Nucl. Chem., Lett.*, **164**, 255 (1992).
42. A. N. Zakharov, B. V. Romanovsky, D. Luka, and V. I. Sokolov, *Organomet. Chem. USSR,* **1**, 64 (1988).
43. A. N. Zakharov, A. G. Gabrielov, B. V. Romanovsky, and V. I. Sokolov, *Vestn. Mosk. Univ., Ser. 2: Khim.*, **30**, 234 (1989).

44. G. Schultz-Ekloff, D. Wohrle, and A. Andreev, *Wiss. Zeitschr. Leuna-Merseburg,* **32**, 649 (1990).
45. R. F. Parton, L. Utytterhoeven, and P. A. Jacobs, *Stud. Surf. Sci. Catal.*, **59**, 395 (1991).
46. R. F. Parton, D. R. C. Huybrechts, Ph. Buskens, and P. A. Jacobs, *Stud. Surf. Sci. Catal.*, **70**, 47 (1991).
47. B. V. Romanovsky and A. G. Gabrielov, *Mendeleev Commun.*, 14 (1991).
48. B. V. Romanovsky and A. G. Gabrielov, *Stud. Surf. Sci. Catal.*, **72**, 443 (1992).
49. B. V. Romanovsky and A. G. Gabrielov, *J. Mol. Catal.*, **74**, 293 (1992).
50 F. Bedioui, E. DeBoysson, J. Devynck, and K. J. Balkus, Jr., *J. Electroanal. Chem., Interfac. Electrochem.*, **315**, 313 (1991).
51. R. Parton, Dissertation, Katholieke Universiteit Leuven (1993).
52. E. Paez-Mozo, N. Gabriunas, F. Lucaccioni, D. D. Acosta, P. Patrono, A. La Ginestra, P. Ruiz, and B. Delmon, *J. Phys. Chem.*, **97**, 12819 (1993).
53. M. Nakamura, T. Tatsumi, and H. Tominaga, *Bull. Chem. Soc. Jpn.*, **63**, 3334 (1990).
54. X. Wang, Y. Liang, Y. Lui, L. Yu, Y. Li, F. Li, and X. Cao, *Gaodeng Xuexiao Hiaxue Xuebao*, **14**, 19 (1993), [CA **119**: 107854j (1993)].
55. C. Bowers and P. K. Dutta, *J. Catal.*, **122**, 271 (1990).
56. K. J . Balkus, Jr., A. A. Welch, and B. E. Gnade, *Zeolites*, **10**, 722 (1990).
57. S. Kowalak, R. C. Weiss, and K. J. Balkus, Jr., *J. Chem. Soc., Chem. Commun.*, 57 (1991).
58. D. E. DeVos and P. A. Jacobs, in *Proceedings from the 9th International Zeolite Conference,* R. Von Ballmoos, J. B. Higgins, and M. M. J. Treacy (Eds), Butterworth-Heinemann, Boston, Vol. 2, pp 615-622 (1992).
59. K. Putyera, G. Plesch, L. Benco, J. Dobrovodsky, A. V. Tchuvaev, V. I. Nefedov, and M. Zikmund, *Proc. 12th Conf. Coord. Chem.*, 295 (1990).
60. F. Bedioui, E. DeBoysson, J. Devynck, and K. J. Balkus, Jr., *J. Chem. Soc., Farad. Trans.*, **87**, 3831 (1991).
61. L. Gaillon, N. Sajot, F. Bedioui, J. Devynck, and K. J. Balkus, Jr., *J. Electroanal. Chem., Interfac. Electrochem.*, **345**, 157(1993).
62. F. Bedioui, L. Roue, L. Gaillon, J. Devynck, S. L. Bell, and K. J. Balkus, Jr., *Petrol. Preprints*, **38**, 529 (1993).
63. K. J. Balkus, Jr., and S. Shepelev, *Micropor. Mater.*, **1**, 383, (1993).
64. K. J. Balkus, Jr., and S. Shepelev, *Petrol. Preprints*, **38**, 512 (1993).
65. G. A. Ozin and C. Gil, *Chem. Rev.*, **89**, 1749 (1989).
66. N. Jaeger, P. Plath, and G. Schultz-Ekloff, *Acta Phys. Chem.*, **31**, 189 (1985).
67. W. M. H. Sachtler, *Acc. Chem. Res.*, **26**, 383 (1993).
68. P. Gallezot, in *Metal Clusters*, E. M. Moskovits (Ed), J. Wiley, New York, pp 219-247 (1986).
69. G. A. Ozin, S. Ozkar, and R. A. Prokopowicz, *Acc. Chem. Res.*, **25**, 553 (1992).
70. W. M. Meier and D. H. Olson, *Atlas of Zeolite Structure Types*, Butterworth-Heinemann, Boston (1992).

71. M. Ichikawa, *Adv. Catal.*, **38**, 283 (1992).
72. L. F. Rao, A. Fukuoka, and M. Ichikawa, *J. Chem. Soc., Chem. Commun.*, 458 (1988).
73. L. F. Rao, A. Fukuoka, N. Kosugi, H. Kuroda, and M. Ichikawa, *J. Phys. Chem.*, **94**, 5317 (1990).
74. N. Takahashi, A. Mijin, H. Suematsu, S. Shinohara, and H. Matsuoka, *J. Catal.*, **177**, 348 (1989).
75. B. E. Hanson, M. E. Davis, D. Taylor, and E. Rode, *Inorg. Chem.*, **23**, 52 (1984).
76. P. Gelin, C. Naccache, and Y. Ben Taarit, *Pure Appl. Chem.*, **60**, 1315 (1988).
77. M. Ichikawa, L. -F. Rao, and A. Fukuoka, *Catal. Sci. Tech.*, **1**, 111 (1991).
78. A. Fukuoka, L. -F. Rao, N. Kosugi, H. Kuroda, and M. Ichikawa, *Appl. Catal.*, **50**, 295 (1989).
79. L. L. Sheu, H. Knozinger, and W. M. H. Sachtler, *Catal. Lett.*, **2**, 129 (1989).
80. L. L. Sheu, H. Knozinger, and W. M. H. Sachtler, *J. Am. Chem. Soc.*, **111**, 8125 (1989).
81. R. S. Drago, I. Bresinska, J. E. George, K. J. Balkus, Jr., and R. J. Taylor, *J. Am. Chem. Soc.*, **110**, 304 (1988).
82. R. J. Taylor, R. S. Drago, and J. E. George, *J. Am. Chem. Soc.*, **111**, 6610 (1989).
83. R. J. Taylor, R. S. Drago, and J. P. Hage, *Inorg. Chem.*, **31**, 253 (1992).
84. I. Bresinska and R. S. Drago, *Stud. Surf. Sci. Catal.*, **69**, 101 (1991).
85. M. Iwamoto, S. -I. Nakamura, H. Kusano, and Sh. Kagawa, *J. Phys. Chem.*, **90**, 5244 (1986).
86. P. -L. Zhou and B. C. Gates, *J. Chem. Soc., Chem. Commun.*, 347 (1989).
87. P. -L. Zhou, S. D. Maloney, and B. C. Gates, *J. Catal.*, **129**, 315 (1991).
88. S. Kawi and B. C. Gates, *J. Chem. Soc., Chem. Commun.*, 702 (1992).
89. S. Kawi, J. -R. Chang, and B. C. Gates, *J. Catal.*, **142**, 585 (1993).
90. R. Nakamura, N. Okada, A. Oomura, and E. Echigoya, *Chem. Lett.*, **119** (1984).
91. A. De Mallmann and D. Barthomeuf, *Catal. Lett.*, **5**, 293 (1990).
92. G. J. Li, T. Fujimoto, A. Fukuoka, and M. Ichikawa, *J. Chem. Soc., Chem. Commun.*, 1337 (1991).
93. G. J. Li, T. Fujimoto, A. Fukuoka, and M. Ichikawa, *Catal. Lett.*, **12**, 171 (1992)
94. G. J. Li, M. Ichikawa, T. Fujimoto, and X. Guo,. *Petrol. Preprints*, **30**, 523 (1993).
95. S. Kawi, J. -R. Chang, and B. C. Gates, *Catal. Lett.*, **10**, 263 (1991).
96. S. Kawi, J. -R. Chang, and B. C. Gates, *J. Phys. Chem.*, **97**, 10599 (1993).
97. T. Bein, S. J. McLain, D. R. Corbin, R. D. Farlee, K. Moller, G. D. Stucky, G. Woolery, and S. Sayers, *J. Am. Chem. Soc.*, **110**, 1801 (1988).
98. S. Kawi and B. C. Gates, *J. Chem. Soc., Chem. Commun.*, 994 (1991).
99. C. Bremard, E. Denneulin, C. Depecker, and P. Legrand, *Stud. Surf. Sci. Catal.*, **48**, 219 (1989).
100. A. G. Gabrielov, K. J. Balkus, Jr., F. Bedioui, and J. Devynck, *Micropor. Mater.*, **2**, 119 (1994).
101. K. J. Balkus, Jr., A. G. Gabrielov, F. Bedioui, and J. Devynck, *Inorg. Chem.*, **33**, 67 (1994).

102. V. J. Frilette and R. W. Maatman, *U. S. Patent 3,373,109* (1968).
103. C. A. Rundell and C. V. McDaniel, *U. S. Patent 3,769,386* (1973).
104. L. A. Rankel and E.W. Valyocsik, *U. S. Patent 4,500,503* (1985).
105. L. A. Rankel and E.W. Valyocsik, *U. S. Patent 4,388,285* (1983).
106. F. Delprato, L. Demotte, J. L. Guth, and L. Huve, *Zeolites*, **10**, 564 (1990).
107. K. J. Balkus, Jr. and S. Kowalak, *U. S. Patent 5,167,942* (1992).
108. K. J. Balkus, Jr., C. D. Hargis, and S. Kowalak, *ACS Symp. Ser.*, **499**, 347 (1992).
109. K. J. Balkus, Jr., S. Kowalak, K. T. Ly, and C. D. Hargis, *Stud. Surf. Sci. Catal.*, **69**, 93 (1991).
110. R. Hoppe, G. Schultz-Ekloff, D. Wöhrle, M. Ehrl, and C. Bräuchle, *Stud. Surf. Sci. Catal.*, **69**, 199 (1991).
111. S. Wohlrab, R. Hoppe, G. Schultz-Ekloff, and D. Wöhrle, *Zeolites*, **12**, 862 (1992).
112. E. W. Valyocsik, *U. S. Patent 4,568,654* (1986).
113. K. J. Balkus, Jr. and S. Shepelev, Unpublished results.
114. K. J. Balkus, Jr., A. D. Sherry, and S. W. Young, *U.S. Patent 5,122,363* (1992).
115. K. J. Balkus, Jr., I. Bresinska, and S. W. Young, in *Proceedings from the 9th International Zeolite Conference,* R. Von Ballmoos, J. B. Higgins, and M. M. J. Treacy (Eds), Butterworth-Heinemann, Boston, Vol. 2, pp 193-201 (1992).
116. D. R. Rolisson, *Chem. Rev.*, **90**, 867 (1990).
117. A. J. Bard and T. E. Mallouk, in *Molecular Design of Electrode Surfaces*, R. W. Murray (Ed), J. Wiley, New York, p 271 (1992).
118. F. Bedioui, L. Roue, E. Briot, J. Devynck, S. L. Bell, and K. J. Balkus, Jr., *J. Electroanal. Chem., Interfac. Electrochem.*, in press.
119. M. G. B. Drew in *Spectroscopic and Computational Studies of Supramolecular Species,* J. E. D. Davies (Ed), Kluwer, Dordrecht, pp 207-237 (1992).
120. P. C. H. Mitchell, *Chem. Ind.* 308, (1991).
121. B. V. Romanovsky, *Acta Phys. Chem.*, **31**, 215, (1985).
122. B. V. Romanovsky, in *Homogeneous and Heterogeneous Catalysis*, I. Y. Ermakov and V. A. Likholobov (Eds), VNU Sci. Press, Utrecht, pp 343-365 (1986).
123. B. V. Romanovsky and A. G. Gabrielov, *Neftekhimiya*, **30**, 617 (1990).
124. C. A. Tolman and N. Herron, *Catal. Today,* **3**, 235 (1988).
125. N. Herron, in *Inclusions Compounds*, J. L. Atwood, J. E. D. Davies, and D. D. MacNicol (Eds), Oxford University Press, Oxford, Vol. 5, pp 90-103 (1991).
126. D. R. C. Huybrechts, R. F. Parton, and P. A. Jacobs, *Stud. Surf. Sci. Catal.*, **60**, 225 (1991).
127. J. Weitkamp, in *Proceedings from the 9th International Zeolite Conference,* R. Von Ballmoos, J. B. Higgins, and M. M. J. Treacy (Eds.), Butterworth-Heinemann, Boston, Vol. 2, pp 13-45 (1992).
128. G. Henrici-Olive and S. Olive, *J. Mol. Catal.,* **1**, 121 (1975-76).
129. R. -J. Wang, T. Fujimoto, T. Shido, and M. Ichikawa, *J. Chem. Soc., Chem. Commum.*, 962 (1992).

130. J. S. Beck, J. C. Vartuli, W. Roth, M. E. Leonowicz, C. T. Kresge, K. D. Schmitt, C. T. -W. Chu, D. H. Olson, E. W. Sheppard, S. B. McCullen, J. B. Higgins, and J. L. Schlenker, *J. Am. Chem. Soc.*, **114**, 10834 (1992).
131. M. Estermann, L. B. McCusker, C. Baerlocher, A. Merrouche, and H. Kessler, *Nature*, **352**, 320 (1991).

Abstract. The various strategies for the preparation of zeolite ship-in-a-bottle complexes are reviewed. Key examples of the cluster, flexible ligand, template and zeolite synthesis methods are described. Evidence for the intrazeolite location of the metal complexes as well as the prevailing interpretation of these results have been organized in terms of the various methods of characterization. A brief summary of known reactivity studies of zeolite encapsulated metal complexes, including catalytic oxidations and hydrogenations, is also presented.